

Document downloaded from:

<http://hdl.handle.net/10251/57093>

This paper must be cited as:

Ruiz Fernández, LÁ.; Recio Recio, JA.; Fernández-Sarría, A.; Hermosilla, T. (2011). A feature extraction software tool for agricultural object-based image analysis. *Computers and Electronics in Agriculture*. 76(2):284-296. doi:10.1016/j.compag.2011.02.007.



The final publication is available at

<http://dx.doi.org/10.1016/j.compag.2011.02.007>

Copyright Elsevier

Additional Information

1 **A FEATURE EXTRACTION SOFTWARE TOOL FOR**
2 **AGRICULTURAL OBJECT-BASED IMAGE ANALYSIS**

3 L.A. Ruiz, J.A. Recio, A. Fernández-Sarría, T. Hermosilla.

4 Departamento de Ingeniería Cartográfica, Geodesia y Fotogrametría, Universidad Politécnica de
5 Valencia, Camino de Vera, s/n, 46022 Valencia, Spain

6 Corresponding author: Luis Ángel Ruiz

7 e-mail address: laruiz@cgf.upv.es

8 Postal address: Departamento de Ingeniería Cartográfica, Geodesia y Fotogrametría

9 Universidad Politécnica de Valencia

10 Camino de Vera, s/n. 46022 Valencia. SPAIN

11 Telephone: 00 34 963877000 ext. 75536

12 Fax Number: 00 34 963877559.

13
14 **ABSTRACT**

15 A software application for automatic descriptive feature extraction from image-objects, FETEX
16 2.0, is presented and described in this paper. The input data include a multispectral high
17 resolution digital image and a vector file in shapefile format containing the polygons or objects,
18 usually extracted from a geospatial database. The design of the available descriptive features or
19 attributes has been mainly focused on the description of agricultural parcels, providing a variety
20 of information: spectral information from the different image bands; textural descriptors of the
21 distribution of the intensity values based on the grey level co-occurrence matrix, the wavelet
22 transform and a factor of edgeness; structural features describing the spatial arrangement of the
23 elements inside the objects, based on the semivariogram curve and the Hough transform; and
24 several descriptors of the object shape. The output file is a table that can be produced in four
25 alternative formats, containing a vector of features for every object processed. This table of
26 numeric values describing the objects from different points of view can be externally used as
27 input data for any classification software. Additionally, several types of graphs and images

28 describing the feature extraction procedure are produced, useful for interpretation and
29 understanding the process. A test of the processing times is included, as well as an application
30 of the program in a real parcel-based classification problem, providing some results and
31 analyzing the applicability, the future improvement of the methodologies, and the use of
32 additional types of data sets. This software is intended to be a dynamic tool, integrating further
33 data and feature extraction algorithms for the progressive improvement of land use/land cover
34 database classification and agricultural database updating processes.

35

36 **Keywords:** feature extraction, parcel-based, image analysis, remote sensing, agricultural
37 database updating, semivariogram, Hough transform, texture.

38

39 1.- INTRODUCTION

40 Image classification techniques are frequently used in remote sensing to face a wide range of
41 applications, being traditionally focused on the analysis of independent pixels using multiple
42 spectral bands as input data, sometimes introducing additional information related to the spatial
43 distribution of the intensity values of the neighbourhood of the pixels, such as the case of the
44 texture based approaches. Much attention has been paid to the process of creating the
45 appropriate decision functions that optimize the accuracy results, and many different
46 methodologies for the classification itself have been tested. However, a crucial step to be taken
47 before the classification is the synthesis of the information or attributes that describe the image
48 element to be classified. This is usually called the feature extraction process, and much less
49 effort has been made in this sense, mainly because the classification has been fundamentally
50 pixel-based, and not object-based, thus restricting the options used to enrich the set of features
51 used as input for the classifiers.

52 *Geographic Object-Based Image Analysis* (GEOBIA) has been defined as a sub-discipline of
53 *Geographic Information Science* devoted to partitioning remote sensing imagery into
54 meaningful image-objects, and assessing their characteristics through spatial, spectral and
55 temporal scale (Hay and Castilla, 2006). Before carrying out feature extraction and
56 classification steps, these techniques require image segmentation. Segmentation refers to the
57 process of partitioning a digital image into multiple segments, called image-objects or simply
58 objects, in order to simplify and/or change the representation of an image into a more
59 meaningful and homogeneous structure that is easier to analyze (Shapiro and Stockman, 2001).
60 These segments have additional spectral and spatial information when compared with single
61 pixels (Blaschke, 2010). Segmentation is the main problem of this analysis of the image because
62 it has multiple solutions (Hay and Castilla, 2006; Zhang et al., 2008). Depending on the method
63 and the parameters used, the results, that are the objects created, can substantially change
64 (Meinel and Neubert, 2004; Neubert and Herold, 2008; Smith and Morton, 2008; Van Coillie et
65 al., 2008). Differing from the automatic image segmentation algorithms, objects can be created
66 using the cartographic limits contained in spatial geodatabases. This approach is known as
67 *Parcel-Based Image Analysis* and has some advantages regarding to other image analysis
68 techniques, the most important being the possibility to directly link the information of the image
69 to the information contained in a database (Berberoglu and Curran, 2004; Walter, 2004).
70 Moreover, for many land use mapping applications, parcel-based classification has been
71 reported to be more accurate than pixel-based classification (Pedley and Curran, 1991; Janssen
72 and Molenaar, 1995; Aplin et al., 1999; Berberoglu et al., 2000; Volante et al., 2007).

73 Once object definition is resolved, the next step is to accurately describe each group of pixels in
74 order to facilitate the correct classification of the object. Different commercial software tools
75 have been made available over the last several years, providing a variety of features to describe
76 the properties of the objects and their mutual relations. These features can be grouped into
77 spectral, textural, shape, thematic attributes, relative to other objects in the same or different
78 segmentation levels and relative to the global image (Baatz et al., 2004). Our need for a tool to

79 automate the descriptive feature extraction process, allowing us to design and incorporate new
80 sets of features describing objects from different perspectives, evaluating and comparing their
81 performance, led us to develop FETEX 2.0, an interactive computer program for image object-
82 oriented feature extraction. The software was written in IDL 6.2 and it can be used on ENVI 4.2
83 or higher. Our aim with this program is to develop new object descriptive features, some of
84 them not included in commercial software tools, designed to characterize specific types of
85 parcels, and with the capacity to adapt certain computation parameters to particular problems.
86 These features can eventually be used with any classifier in order to assign a class to each
87 object. The software requires, as input data, images and vectorial files containing the polygon
88 boundaries in ESRI shapefile (shp) format.

89 FETEX 2.0 does not include any segmentation algorithm, but it creates the objects according to
90 the limits contained in the vectorial file. From each one of the objects created, spectral, textural,
91 shape and structural features can be extracted. The structural features provide information about
92 the distribution of elements inside each object, detecting and quantifying possible spatial
93 patterns, very often relevant in identifying the land use/land cover of objects, especially when
94 working in agricultural areas. For each object, the output is a feature vector ready to be used
95 with the selected classifier. Information obtained with FETEX 2.0 can be used not only in the
96 classification of the database objects, but also as ancillary information in agricultural
97 inventories. Such ancillary information can be the number of trees in a parcel, their average size,
98 planting distances, etc. Additional images and explanatory graphs about the features extracted
99 that may be useful for interpretation of results can be obtained as well.

100 FETEX 2.0 is designed to work with land use/land cover databases in order to help in the
101 process of classification of the existing parcels, or also to determine the changes that have
102 occurred in a database comparing the current classified image with the old database. It has been
103 applied successfully in the feature extraction phase in several updating land use/land cover
104 cartography processes (Ruiz et al., 2009). Interested users are most likely to be among the
105 cartographic research community and official cartographical institutions devoted to updating

106 and maintaining large land use/land cover databases. A limited version of FETEX 2.0 is
107 available at the Geo-Environmental Cartography and Remote Sensing Research Group (CGAT)
108 website (<http://cgat.webs.upv.es>).

109

110 **2.- EXTRACTION OF DESCRIPTIVE FEATURES WITH FETEX 2.0**

111 The main reason for developing the program was to create a tool for supporting the process of
112 classification and updating of land use/land cover spatial databases from an object-based
113 perspective. The extraction of valuable features for this process is essential. FETEX 2.0 is
114 designed to independently process each image-object to extract a variety of descriptive features
115 useful to characterize the current land use/land cover. These features can be grouped into five
116 categories: spectral, textural, structural, shape and those extracted from ancillary data. In this
117 section, the features are briefly described or referenced.

118 **2.1.- Spectral features**

119 Spectral features provide information about the spectral response of objects, which depends on
120 land coverage types, state of vegetation, soil composition, construction materials, etc. These
121 features are especially useful in the characterization of spectrally homogeneous objects, such as
122 herbaceous crops, fallow fields or compact industrial areas. This group of features constitutes
123 the traditional information derived from any type of multispectral imagery. In addition to the
124 original spectral bands, any combination, ratio, or transformation (principal components,
125 tasselled cap bands, etc) can be included as complementary bands in the input raster file to be
126 processed.

127 For each band contained in the input raster file, the values of mean, standard deviation,
128 minimum, maximum, range, sum and majority of the pixel values inside each object can be
129 calculated.

130 **2.2.- Texture features**

131 The texture informs about the spatial distribution of the intensity values in the image, providing
132 information about contrast, uniformity, rugosity, regularity, etc. A considerable number of
133 quantitative texture features and approaches have been reported using different methodologies.
134 Traditionally, they are computed considering the neighbourhood of each pixel on the image. In
135 our case, each texture feature value is referred to a particular object, since it is extracted from
136 each group of pixels that constitute an object. The simplest manner to characterize texture is
137 based on the first order histogram features. Features such as *kurtosis* and *skewness*, representing
138 the distribution of values of the histogram of an object, are included in FETEX 2.0. The most
139 widely used set of features is that proposed by Haralick et al. (1973), based on the grey level co-
140 occurrence matrix (GLCM) and also called second order histogram features. Up to seven of these
141 features can be extracted by FETEX 2.0: *contrast*, *uniformity*, *entropy*, *variance*, *covariance* or
142 *product moment*, *inverse difference moment*, and *correlation*. Since an object-oriented approach
143 is used, only one GLCM is computed for each object, describing the co-occurrences of the pixel
144 values that are separated at a distance of one pixel inside the polygon, and considering the
145 average value of four principal orientations (0°, 45°, 90° and 135°) in order to avoid the
146 influence of the orientation of the elements inside the objects, keeping in mind a potential
147 classification process. Therefore, only one value for every GLCM feature is computed for each
148 object. Although the *mean* of the GLCM is one of the most widely used features in texture
149 image classification problems at the pixel level, due to its very high correlation to the mean
150 value of the original band, this feature has been intentionally excluded from the set of GLCM
151 features.

152 Another powerful feature is the *edgeness factor*, that represents the density of edges present in a
153 neighbourhood. Sutton and Hall (1972) proposed the following formula to compute the
154 *edgeness factor* g :

$$g(d) = \sum_{(i,j) \in N} \{ |I(i,j) - I(i+d,j)| + |I(i,j) - I(i-d,j)| + |I(i,j) - I(i,j+d)| + |I(i,j) - I(i,j-d)| \} \quad (1)$$

155 where g is computed as a function of the distance d between pixels of an image I in a
156 neighbourhood N . Due to the good performance of this feature in different landscape
157 classification problems (Ruiz et al., 2002; 2004), it has been included in the program, and the
158 *mean* and the *standard deviation* of the *edgeness factor* for each parcel is computed.

159 **2.3.- Wavelet-based texture features**

160 Although the basic ideas of wavelets existed since the beginning of last century, the applied
161 mathematical models were developed in the mid-eighties. A review and mathematical
162 description of wavelets can be found in Bultheel (1995), and Walker (1999). The use of the
163 wavelet transform for texture analysis was first proposed by Mallat (1989). Since the texture of
164 an image is a function of the scale, an advantage of wavelet decomposition is that it provides a
165 unified framework for multiscale analysis. The wavelet transform allows for the decomposition
166 of a signal using a series of elemental functions called *wavelets* and *scaling*, which are created
167 by the scaling and translation of a base function, known as the *mother wavelet*:

$$\psi_{s,u} = \frac{1}{\sqrt{s}} \psi\left(\frac{x-u}{s}\right), \quad s \in \mathfrak{R}^+, \quad u \in \mathfrak{R} \quad (2)$$

168 where s governs the scaling and u the translation. The wavelet decomposition of a function is
169 obtained by applying each of the elemental functions or wavelets to the original function:

$$Wf(s,u) = \int_{\mathfrak{R}} f(x) \frac{1}{\sqrt{s}} \psi^*\left(\frac{x-u}{s}\right) dx \quad (3)$$

170 In the practice of image analysis, the extension to a 2-D discrete function is usually performed
171 by means of a product of 1-D low-pass and high-pass filters. As a result, the wavelet transform
172 decomposes the original image into a series of images with different scales, called trends and
173 fluctuations. The former are averaged versions of the original image, and the latter contain the
174 high frequencies at different scales or levels. Since the most relevant texture information is lost
175 in the lowpass filtering process, only fluctuations are used to calculate texture descriptors. If the

176 inverse transform is applied to the fluctuations, three reconstructed images, or *details*, are
177 obtained: horizontal, vertical and diagonal. This process is called multiresolution analysis.

178 Different texture features have been extracted from wavelet details or fluctuations, such as the
179 local energy (Randen and Husoy, 1999), variance filter (Ferro and Warner, 2002), histogram
180 signatures (Simard et al., 1999), or co-occurrence features (Van de Wouwer et al., 1999; Ruiz et
181 al., 2004).

182 The application FETEX 2.0 includes some texture features based on the wavelet transform.
183 Seven families of wavelet functions (Haar, Daubechies, Coiflet, Meyer, Symlet, Shannon and
184 Battle-Lemarié) can be applied over the image objects. Defining the support of a wavelet
185 function as the smallest closed interval, outside of which the function is zero (Bultheel, 1995),
186 different supports have been defined for each wavelet family, following the work of Fernández-
187 Sarría (2007). A total of eight Haralick's features derived from the GLCM can be extracted
188 from the image containing the sum of the reconstructed details (*mean, contrast, uniformity,*
189 *entropy, variance, covariance, inverse difference moment, and correlation*), as well as the *mean*
190 *and standard deviation* of the *edgeness factor*.

191 However, applying the wavelet transform using an object-oriented approach may be a problem
192 when large supports are used, since a higher proportion of neighbour pixels located outside the
193 analyzed object will be considered in the transformation process. Two measures are followed to
194 reduce this effect: First, an erosion filter using a circular structuring element with a diameter
195 size equal to the support of the wavelet function is applied to the final image. A limitation of
196 this is that small and/or narrow objects will be completely eroded, and subsequently omitted
197 from the characterization of the features that belong to this group. Secondly, even if up to three
198 levels of decomposition are included for computation in FETEX, only the first level is enabled
199 in the current version, in order to avoid the decimation of the image to the point that the object
200 practically disappears when the direct transform is applied. This effect will be negligible when
201 working with large objects.

202 **2.4.- Structural features**

203 Structural features provide information of the spatial arrangement of different elements in the
204 object, in terms of randomness or regularity of the distribution of the elements. This is the case
205 of alignments or regular patterns that are present in different man-made landscapes, such as the
206 planting patterns of crops and trees in agricultural plots (Recio et al., 2006; Ruiz et al., 2007).
207 The identification of regular planting patterns can be particularly useful in agricultural
208 classification, as reported by several authors (Trías-Sanz, 2006; Helmholtz et al., 2007; Ruiz et
209 al., 2009; Recio, 2009; Hermosilla et al., 2010). Structural features computed in FETEX 2.0 are
210 divided into two groups: the semivariogram and the Hough transform derived features.

211 **2.4.1.- Features extracted from the experimental semivariogram**

212 The semivariogram quantifies the spatial associations of the values of a variable, and measures
213 the degree of spatial correlation between different pixels in an image. This is a particularly
214 suitable tool in the characterization of regular patterns. The expression which describes the
215 experimental semivariogram of a continuous variable is:

$$\gamma(h) = \frac{1}{2N} \sum_{i=1}^N [z(x_i) - z(x_i + h)]^2 \quad (4)$$

216 where $z(x_i)$ represents the value of the variable in position x_i , N is the number of pairs of data
217 considered and h provides the separation between elements in a given direction.

218 The semivariogram has been widely employed in digital image processing. Its usefulness in
219 remote sensing has been demonstrated, complementing the spectral variables with information
220 related to the spatial structure of the image (Carr, 1996; Durrieu et al., 2005). The relationship
221 between the range of the semivariogram and the size of the pattern described by the objects of
222 an image has been studied by Woodcock et al. (1988a, 1988b). Carr and Miranda (1998) used
223 the slope in the origin as a feature directly related to the variability of the intensity values in
224 these objects. Other works are focused on the extraction of descriptive features from the

225 semivariogram of remotely sensed images. Thus, Chica-Olmo and Abarca-Hernandez (2000)
226 computed the first value of that function in the neighbourhood of a pixel to characterize the
227 texture of that neighbourhood. Maillard (2003) used all the semivariogram values, conferring
228 more importance to the initial values, and less to the subsequent values. These and other authors
229 (Jakomulska and Clarke, 2000; Ashoori et al., 2008; etc.) used different features extracted from
230 the semivariogram computed in a window around a pixel in order to perform a classification.

231 The omnidirectional semivariogram can be obtained by averaging the semivariograms of all
232 possible directions. However, this approach requires a long processing time. This
233 semivariogram is obtained in FETEX 2.0 by computing, for each object, the mean of the
234 semivariograms calculated in six different directions, ranging from 0° to 150° with a step of 30°.
235 Afterwards, each semivariogram curve is smoothed using a Gaussian filter with a stencil of 3
236 positions, in order to reduce experimental fluctuations.

237 In homogeneous objects, semivariance values tend to be higher as the lag increases. However,
238 when the elements inside an object are spatially arranged following a regular pattern, the
239 semivariogram has a cyclic behaviour, and it is known as *hole-effect semivariogram* (Pyrcz and
240 Deutsch, 2003). This type of behaviour is common in areas with a high level of human
241 intervention, such as certain crops, urban or industrial landscapes. Figure 1 shows the
242 experimental semivariogram curves of four parcels with different land uses. Figure 1a and
243 Figure 1c present parcels containing tree crops that follow regular plantation patterns, their
244 semivariograms being examples of *hole-effect semivariograms*. On the other hand, Figure 1b
245 and Figure 1d do not present regular patterns or spatial cyclicity, and their semivariogram
246 curves follow a monotonous rising trend.

247 The features extracted by FETEX 2.0 are based on the zonal analysis defined by a set of
248 singular points on the semivariogram, such as the first maximum, the first minimum, the second
249 maximum, etc., and are fully described in Balaguer et al. (2010). The semivariogram derived
250 features are: *ratio variance at first lag*, *ratio between semivariance values at second and first*

251 *lag, first derivative near the origin, lag value corresponding to the first maximum, mean of the*
252 *semivariogram values up to the first maximum, variance of the semivariogram values up to the*
253 *first maximum, area between the semivariogram value in the first lag and the semivariogram*
254 *function until the first maximum, ratio between the semivariance at first local maximum and the*
255 *mean semivariogram values up to this maximum, distance between the location of the first local*
256 *maximum and the second local maximum, and distance between the first maximum and the first*
257 *minimum.*

258 In terms of efficiency in processing time, instead of computing the semivariogram considering
259 all the pixels inside each object, only a random selection of pixels is used, in order to reduce the
260 processing time. A test was carried out in order to assess the influence of the percentage of
261 pixels used in two processes: in the calculation of the semivariogram curve, and in the
262 performance of the classification of a sample of N objects. The results show that
263 semivariograms calculated using a reduced number of random pixels are very similar to those
264 computed using all the pixels inside each object, as shown in the two examples of Figure 2.

265 Regarding the classification performance, Figure 3 shows a graph representing the overall
266 accuracies obtained in a per-object classification using the set of features derived from the
267 semivariogram described above. Ten classification processes have been compared. In each, a
268 different percentage of pixels has been randomly selected for semivariogram calculation. The
269 overall accuracy obtained using 100% of the pixels is 81.3%. The results reveal that the
270 semivariogram derived features computed when using only 15% of the pixels describe the
271 objects with an efficiency similar to that of when all the pixels are used, since they do not
272 produce a significant reduction in the classification accuracy. Besides, the processing time is
273 linearly reduced: 85% using only 15% of pixels, 75% considering a 25% and so on.

274 **2.4.2.- Features derived from the Hough transform**

275 The planting pattern and planting distances are key factors employed by photointerpreters to
276 distinguish different crop typologies. Thus, once the information about global regularity of the

277 parcel is extracted from the semivariogram analysis, the plantation pattern can be more
278 profoundly analysed in order to obtain more specific descriptors that complement the
279 semivariogram derived features. For this purpose, a variety of features based on the Hough
280 transform are included in FETEX 2.0.

281 The first step in the extraction of these features is the location of trees, which is done using the
282 local maximum filtering (LMF) method (Gourgeon, 1999) from high spatial resolution imagery.
283 The LMF is based on the assumption that reflectance is highest at the tree apex and decreases
284 towards the crown edge (Wulder et al., 2000). Moving a kernel over the image, trees are found
285 when the central value in the kernel window is higher than all other values. The scene
286 illumination has an important influence on local maxima position, displacing their position from
287 the real apex location. However, this displacement has no negative effects because it equally
288 affects all the maxima.

289 LMF method is applied over NDVI images using a circular kernel with variable size to detect
290 adult trees. This size is automatically determined for each object by the position of the first
291 maximum on the semivariogram curve, being constrained by the interval defined between two
292 thresholds that are set by the user. If the first maximum is lower than the lower threshold, this
293 threshold will be used as the diameter of the kernel. In a similar way, if the first maximum is
294 greater than the upper threshold, the diameter of the kernel will be the upper threshold.
295 Assuming a regular distribution of trees in a parcel, the kernel diameter is related to the average
296 size of the trees contained in a parcel.

297 Most of these features are designed for the classification of agricultural tree orchards. In order to
298 facilitate this task, two main groups of trees can be considered: adult trees, having a
299 considerable canopy, and young trees, with almost no vegetation cover. A threshold defined
300 over the NDVI image is selected in order to distinguish those two groups of parcels. In those
301 parcels with a NDVI mean value lower than the defined threshold, instead of applying LMF
302 over the NDVI image, trees are searched by using a local minimum filtering (LmF) over the

303 infrared (IR) band. This variation is used in order to locate the young trees recently planted. The
304 result is a binary image where each located tree is represented by a pixel. In both cases, adult
305 and young trees, pixel location must accomplish an additional condition: the maximum in NDVI
306 band must be greater than a threshold fixed by the user and the minimum in IR band must be
307 lower than a threshold, which must be empirically defined depending on the image
308 characteristics. From this binary image, main tree alignments are extracted and characterized
309 applying the Hough transform (Hough, 1962).

310 The **Hough transform** is a method that can be used in image processing to locate curves that
311 can be parameterized as straight lines, polynomials or circles. This method has been widely
312 used on images for row detection in agricultural crops (Reid and Searcy, 1986; Leemans and
313 Destain, 2006; Gée et al., 2008). Structural information derived from the Hough transform has
314 also been used for automatic classification and characterization of agricultural landscapes.
315 Chanussot et al. (2005) applied the Fourier transform over a vineyard image, and then, the
316 Hough transform for estimating and representing the crop orientation. Trias-Sanz (2006)
317 employed structural properties based on orientation features to discriminate between different
318 vegetation covers. He applied the variogram transformation and then, over the resultant image,
319 the Hough transform, obtaining the orientation histogram. Helmholtz et al. (2007) used the
320 orientation information directly derived from the Hough transform to separate between tilled
321 and untilled plots based on the existence of a minimum number of parallel lines.

322 The principle of the Hough transform is based on the fact that an infinite number of straight
323 lines can go through a single point of the plane. The purpose of the method is to determine
324 which of these theoretical lines go through more points in the image, that is, to find the best
325 fitting lines to the set of points that are present in the image. The method is based on the
326 transformation of the coordinates from a Cartesian image space to a polar coordinate space. A
327 point in the Cartesian space corresponds to a sinusoid in the polar space, representing the
328 parameters of the lines passing through that point. A line in the Cartesian space is defined by the
329 intersection of two or more sinusoids in the polar space.

330 After thresholding the polar space to remove lines passing through a small number of points,
331 remaining lines are grouped into a histogram of frequencies for all directions ranging from 0° to
332 180°. When some regularity in their spatial arrangement exists, two histogram maxima appear,
333 corresponding to the principal directions or alignments of trees in the parcel. Figure 4 shows an
334 example of this: a tree parcel (Figure 4a); the binary image with the local maxima representing
335 the location of trees, with the orientations of the two principal alignments superimposed (Figure
336 4b); the result of the Hough transform (Figure 4c). The existence of points where several curves
337 converge indicates the presence of alignments in the Cartesian domain. Grouping these values
338 in a histogram of frequencies, the two orientations of the principal alignments in the parcel are
339 easily differentiated at 75° and 161° (Figure 4d). By isolating these orientations, the angular
340 difference between them provides information about the orthogonality of the alignments. The
341 distance between the points where the curves converge on the same direction in the Hough
342 domain correspond to the distance between the lines following that direction. These distances
343 are used to describe the planting pattern size of tree crops along the two main orientations
344 (Figure 5).

345 A set of additional features related to the regularity in the distribution of trees are extracted from
346 this transformation and the histogram of orientations. These features are: *proportion of points*
347 *included in the principal and secondary direction with respect to the total amount of points;*
348 *mean, median and standard deviation of the distances between straight lines in the principal*
349 *and secondary directions; proportion of straight lines in the principal and secondary*
350 *directions; and angular difference between the two principal directions.*

351 **2.5.- Shape features**

352 The shape features computed in FETEX 2.0 inform about the shape complexity of the objects,
353 and are mainly based on ratios between the area and the perimeter of the objects. These
354 descriptors, extracted directly from the geometric definition of the polygons contained in the

355 database (parcels) can help to distinguish and identify different elements with particular shapes,
356 such as roads, rivers, circular plots, etc.

357 The features available in the application are: *compactness* (Bogaert et al., 2000), *shape index*
358 and *fractal dimension* (Krummel et al., 1987; McGarigal and Marks, 1995) (see Table 1). The
359 area and perimeter of each object are also computed.

360 **2.6.- Ancillary data**

361 Depending on the algorithm used in a subsequent classification process, discrete variables can
362 be included as descriptive features. Some studies (Rogan et al., 2003; Recio et al., *in press*) have
363 shown that the combination of the historical land use of the parcels contained in an old database
364 with spectral features may increase the overall accuracy of the classification. Some other
365 discrete information, such as soil type and composition (Huang and Jensen, 1997), irrigation
366 type, etc. can sometimes be useful to better describe the parcels or polygons. If this information
367 is included in the spatial geodatabase as an input in FETEX 2.0, it can also be added as an
368 output to the descriptive feature vector of each parcel.

369 Any other georeferenced information in raster format can also be added as extra input to extract
370 information and characterize the objects. Thus, digital terrain models (elevation, slope or aspect)
371 (Hoffer, 1975; Hutchinson, 1982), distance maps (Debeir et al., 2002; Mas, 2003; Recio et al.,
372 2010), results of a *per-pixel* classification (Recio, 2009) or others, can be added as additional
373 bands in order to compute statistics to describe the parcels.

374

375 **3.- THE PROGRAM**

376 **3.1.- Graphic User Interface**

377 The Graphic user interface of FETEX 2.0 is a window menu divided in five frames (Figure 6):
378 1.- Input files, 2.- Output files, 3.- Feature selection, and 4.- Feature parameters definition.

379 **3.1.1.- Input files**

380 Image formats supported by FETEX 2.0 must be georeferenced and are those supported by
381 ENVI (GeoTIFF, JPG2000, ENVI binary, ERDAS img, etc.). Limits of cartographic objects
382 (parcel) must be contained in a ESRI shapefile spatial data format (.shp). In order to correctly
383 superimpose both data, the image and the shapefile, they should be in the same spatial reference
384 system.

385 FETEX 2.0 is able to work with large datasets of several images and shapefiles. In the case that
386 a parcel (object) is represented along several image files, the program will internally build a
387 mosaic and extract the final descriptive features from this new composed image.

388 **3.1.2.- Output files**

389 As a result of processing the image for object information extraction, an output table containing
390 the values of the descriptive features selected (columns) for every object processed (rows) is
391 obtained. This table can be available in four different formats: dBase, shapefile, ASCII and the
392 format required by See5 software, which contains the C5.0 algorithm to generate decision trees.

393 In addition to the table with all the feature values needed for the classification of the objects,
394 FETEX 2.0 provides the option of generating a set of screenshots and graphs that may be
395 helpful for the interpretation of the results (Figure 7). The set of screenshots obtained for every
396 object includes a color or grey level image of the object, the image of the wavelet details, image
397 files of the GLCM of the original image and the wavelet details, the semivariogram graph, a
398 binary image of the tree locations automatically detected, its Hough transform graph, and the
399 binary image of the tree alignments. Additionally, a dbf file containing the semivariogram for
400 each analyzed object can be generated.

401 **3.1.3.- Feature selection**

402 In this frame, the user can select the groups of features to be extracted from the objects. There
403 are seven main groups of features: spectral, texture features based on the GLCM, wavelet

404 derived texture features, descriptive parameters derived from the semivariogram, Hough
405 transform based features, shape features, and qualitative features from a database.

406 On the right side of the frame, there are three drop-down lists for the selection of the image
407 bands from which the GLCM, wavelet and semivariogram features will be computed.

408 The last item in this menu enables us to use descriptive information from the input shapefile
409 database as an additional descriptive feature. If the *Database feature* option button is enabled,
410 the field of the shapefile database containing the descriptive feature must be selected from the
411 adjoining drop-down list.

412 **3.1.4.- Feature parameters definition**

413 This frame is divided in three sections. In the first section, three general parameters of the
414 process can be fixed: *Minimum parcel size* controls the minimum area of a polygon to be
415 processed, avoiding very small polygons that may difficult a correct characterization. *Parcel*
416 *perimeter buffer* is used to reject the peripheral pixels of the polygon in the analysis, in order to
417 avoid the inclusion of pixels that are external to the object due to geo-referencing errors or
418 misregistration between the database and the image. The values of the droplist represent the
419 thickness of the rejecting buffer in pixels. *NDVI bands* droplist allows for the selection of the
420 two image bands required for computing the NDVI: the IR and red bands.

421 The second section of this frame (*Analysis options*) allows for the selection of the specific
422 features that can be obtained from the different feature groups, as well as the methodological
423 parameters involved.

424 In the first tab, seven statistical features can be selected to be computed from each object. These
425 features are computed for every band of the input image.

426 The second tab corresponds to the texture features. The number of grey levels to be considered
427 in the computation of the GLCM can be chosen. The selection of this parameter is important,
428 because the use of many grey levels does not necessarily mean an increase in the efficiency of

429 the descriptors, but greatly increases the time consumed for computation. Furthermore, in
430 objects containing a low number of pixels, many grey levels in the computation of the GLCM
431 can make the characterisation of the distribution of the values in the matrix difficult.

432 The wavelet tab controls the wavelet function family and the support used to perform the
433 wavelet transform. Higher support values will require longer processing time. The number of
434 grey levels to be considered in the computation of the GLCM can also be chosen.

435 Two parameters can be controlled in the semivariogram tab: the *maximum Semivariogram lag*
436 *size*, and the *Percentage of pixels* from an object that are used to estimate its semivariogram, as
437 analyzed at the end of section 2.4.1.

438 In the Hough transform tab, several thresholds related to the automatic process to detect the
439 trees inside a parcel can be established. The *Initial NDVI (parcel)* parameter allows for the
440 definition of a threshold for the mean NDVI of the object. For those objects with a mean NDVI
441 higher than this value, the LMF method is applied using the NDVI image to locate the trees. On
442 the other hand, for the objects with a mean NDVI lower than this threshold value, the trees are
443 located applying the LmF method using the IR band. Afterwards, two conditional thresholds
444 must be established: those pixels located with the LMF method must have a NDVI value higher
445 than the *NDVI threshold* to be accepted as a tree, whereas the IR band values of the pixels
446 located with the LmF method must be lower than the *IR band threshold*.

447 Additionally, a selection of the threshold values used to define the size of the searching window
448 must be done, specifically the minimum and maximum *Window diameter* values. These values
449 must be in concordance with the minimum and maximum sizes of the trees, in pixels, that are
450 present in the specific geographic area.

451 The last tab corresponds to the selection of the shape features to be computed.

452 The last part of this frame (*Attributes in the shapefile*) first allows for the selection of the object
453 identifier field in the shapefile of the database (*ID*), which must be an integer number. In

454 addition to this, when a field containing the class of the training samples exists in the database,
455 this can be selected in the last drop-down list (*Samples*). This information will be added at the
456 end of the row of the feature vector corresponding to each object. The parcels that are not
457 training samples will have a question mark at the end of the row. This field is required in order
458 to obtain a *See5* file format output.

459 **3.2 Future improvements**

460 FETEX 2.0 has been designed to work with large datasets, including images and shapefiles. In
461 addition, some effort has been put to reduce the time needed to compute the different procedures
462 used in the program, this is particularly important when a high number of objects must be
463 processed.

464 The program allows for the extraction of a wide range of features from images and databases,
465 some of them mainly focused on agricultural landscapes, with the final goal of describing the
466 objects in depth in order to improve their classification. However, the program is intended to be
467 a dynamic tool that progressively incorporates new feature extraction algorithms, as well as
468 different types of spatial data which are currently more widely available,. The design and
469 analysis of new descriptive features coming from different sources of information (airborne
470 lidar systems, satellite radar images, etc.) will continue in order to advance in the description of
471 objects. Useful three-dimensional information about the objects and the elements they may
472 contain can be extracted from lidar data, complementing the current information available. In a
473 different way, high resolution radar imagery can provide extra information about the roughness
474 of the surfaces, which may complement the previous features. All these new sources of
475 information are becoming more widely available to the user, and new tools to integrate and
476 process the data will be needed.

477

478 **4.- APPLICATION EXAMPLE: OBJECT-ORIENTED CLASSIFICATION OF** 479 **AN AGRICULTURAL DATABASE**

480 An object-oriented classification application example has been carried out using the descriptive
481 features extracted with FETEX 2.0. The test has been performed using data from a rural area in
482 the province of Castellón, on the Mediterranean coast of Spain. A series of aerial images
483 acquired in August 2005 with a Digital Mapping Camera (DMC) have been used, with a spatial
484 resolution of 0.5 m/pixel and three spectral bands (green: 0.50-0.65 μm ; red: 0.59-0.675 μm ;
485 and near infrared: 0.675-0.85 μm). A total of 616 training samples and 2438 evaluation samples
486 have been selected from the cadastral polygons. The reference data used for evaluation have
487 been obtained combining field work and photointerpretation. According to the type of
488 landscape, ten different classes have been defined in the classification: *Arable fields*, *Buildings*,
489 *Carob-trees*, *Citrus orchards*, *Irrigated fields*, *Olive trees*, *Roads*, *Shrub-lands*, and *Young*
490 *citrus orchards*. Figure 8 shows some image-object examples of each class.

491 A set of different descriptive features has been computed using FETEX 2.0. They can be
492 grouped as follows: (1) Spectral features: Mean, standard deviation, minimum and maximum
493 from each band, and NDVI; (2) Texture features: GLCM derived features, *edgeness factor*, 1st
494 order descriptors, and wavelet based features computed from the red band; (3) Structural
495 features: Hough transform and semivariogram derived features computed from the infrared
496 band; and (4) Shape features.

497 Two classification methods have been used: Linear discriminant analysis (LDA), and decision
498 trees computed using the C5.0 algorithm and combined with the boosting multi-classifier
499 method. The classifications obtained have been evaluated by means of the error matrix
500 (Congalton, 1991), from which the overall accuracy rate, the user's and producer's accuracies
501 for every class have been computed.

502 Four tests per classification method have been done to independently evaluate the performance
503 of each descriptive feature group. An additional classification has been performed combining all
504 features. Table 2 shows the overall classification accuracies obtained using the different groups
505 and combinations of descriptive features. In both classification methods, the use of all the

506 features from the different groups together sharply increases the overall accuracy rate of the
507 classification. Additionally, no significant differences in overall accuracy are found between
508 both methods when all the feature groups are used, showing that the influence of the classifier is
509 not crucial when an exhaustive and complementary set of descriptive features is used. However,
510 the use of independent sets of features may introduce some differences in the overall accuracy
511 depending on the classification method used. Thus, using only spectral features, LDA provides
512 a better accuracy (65.5%) than decision trees (60%), but the latter increases the accuracy
513 (62.1%) with respect to the LDA method (57.8%) when only structural features are included for
514 classification. These differences may be due to the fact that the distribution of values of the two
515 groups of features, spectral and structural, are subject to specific ranges, and both classification
516 methods manage this information in different manner.

517 In order to study the influence or discriminant power that the variables (descriptive features)
518 have on the classification, two approaches have been employed: forward stepwise LDA and the
519 comparison of the percentage of use of each specific variable in all the decision trees created
520 using the method of boosting. Figure 9 shows the per-class average of user's and producer's
521 accuracies, and the overall classification accuracy when the 24 first features are progressively
522 included in the discriminant model. Figure 10 shows the percentage of use for the 24 descriptive
523 features most used by the classifier over the training objects.

524 The shape feature *fractal dimension* is the most frequently used in the decision trees and the
525 first discriminant feature selected in the stepwise LDA, allowing for the discrimination of class
526 *Roads* very efficiently, due to the characteristic long shape of the polygons that represent this
527 class. Particularly interesting is the fact that, always, some variables coming from the four
528 different groups considered are selected among the most relevant features. Using this short
529 group of variables the overall accuracy becomes stable, independently of the inclusion of
530 additional variables in the classification set (Figure 9). This illustrates again their
531 complementarity, as well as the possibility to increase the efficiency of the classification not

532 only in terms of accuracy, but also in terms of reduction of the number of variables to be used,
533 by using only a selected group of features with low correlation.

534

535 **5.- SUMMARY**

536 A software program, FETEX 2.0, that extracts a set of descriptive features from image-objects
537 and geodatabases is presented. A description of the features, classified into seven different
538 groups and providing different and complementary information about the object, is carried out.
539 Some of them are particularly useful to characterize and classify agricultural landscapes and
540 have been presented for the first time here.

541 This software application generates an output table containing the object feature vectors
542 available in different formats, ready to use with different classifiers included in statistical
543 packages. Additionally, different types of descriptive graphs and images can be obtained to
544 facilitate the interpretation of processes and results. A classification example has been
545 performed, showing the wide range of information obtained from each object. In this application
546 example, it has been shown how the use of different types of variables provides a complete
547 description of the object, increasing the accuracy of the land use/land cover classification. The
548 software program presented here allows for the computation of all these variables for their
549 application to object-oriented classification, particularly interesting for agricultural mapping.

550 FETEX 2.0 can be considered to be a dynamic program in a continuous updating process in
551 order to incorporate new sources of data, new methods and features, and with the ability to be
552 oriented to specific applications. A limited version of FETEX 2.0 is available at the Geo-
553 Environmental Cartography and Remote Sensing Research Group (CGAT) website
554 (<http://cgat.webs.upv.es>).

555

556 **6.- ACKNOWLEDGMENTS**

557 The authors appreciate the financial support provided by the Spanish Ministerio de Ciencia e
558 Innovación and the FEDER in the framework of the Project CGL2009-14220 and CGL2010-
559 19591/BTE, the Spanish *Instituto Geográfico Nacional (IGN)*, *Instituto Cartográfico*
560 *Valenciano (ICV)*, *Instituto Murciano de Investigación y Desarrollo Agrario y Alimentario*
561 *(IMIDA)* and *Banco de Terras de Galicia (Bantegal)*.

562

563 REFERENCES

564 Aplin, P., Atkinson, P.M., Curran, P.J., 1999. Per-field classification of land use using the
565 forthcoming very fine spatial resolution satellite sensors: problems and potential solution. In:
566 Atkinson, P.M., Tate, P.M. (Eds.) *Advances in Remote Sensing and GIS Analyses*, Wiley &
567 Son, Chichester, pp. 219-239.

568 Ashoori, H., Fahimnejad, H., Alimohammadi, A., Soofbaf, S.R., 2008. Evaluation of the
569 usefulness of texture measures for crop type classification by hyperion data. *International*
570 *Archives of the Photogrammetry, Remote Sensing and Spatial Information Sciences XXXVII-*
571 *B8*, 999-1006.

572 Baatz, M., Benz, U., Dehghani, S., Heynen, M., Höltje, A., Hofmann, P., Lingenfelder, I.,
573 Mimler, M., Sohlbach, M., Weber, M., Willhauck, G., 2004. *eCognition USER GUIDE 4* on
574 CD.

575 Balaguer, A., Ruiz, L.A., Hermosilla, T., Recio, J.A., 2010. Definition of a comprehensive set
576 of texture semivariogram features and their evaluation for object-oriented image classification.
577 *Computers & Geosciences* 36 (2), 231-240.

578 Berberoglu, S., Curran, P. J., 2004. Merging spectral and textural information for classifying
579 remotely sensed images, In: De Jong, S.M., Van der Meer, F.D. (Eds.) *Remote Sensing Image*
580 *Analysis: Including the Spatial Domain*, Kluwer Academic Publishers, Dordrecht, pp. 113-136.

581 Berberoglu, S., Lloyd, C.D., Atkinson, P.M., Curran, P.J., 2000. The integration of spectral and
582 textural information using neural networks for land cover mapping in the Mediterranean.
583 *Computers & Geosciences* 26 (4), 385-396.

584 Blaschke, T., 2010. Object based image analysis for remote sensing. *ISPRS Journal of*
585 *Photogrammetry and Remote Sensing* 65 (1), 2-16.

586 Bogaert, J., Rousseau, R., Hecke, P. V., Impens, I., 2000. Alternative area-perimeter ratios for
587 measurement of 2D shape compactness of habitats. *Applied Mathematics and Computation* 111
588 (1), 71-85.

589 Bultheel, A., 1995. Learning to swim in a sea of wavelets. *Bulletin of the Belgian Mathematical*
590 *Society* 2 (1), 1-46.

591 Carr, J.R., 1996. Spectral and textural classification of single and multiple band digital images.
592 *Computers & Geosciences* 22(8), 849-865.

593 Carr, J.R., Miranda, F.P., 1998. The semivariogram in comparison to the co-occurrence matrix
594 for classification of image texture. *IEEE Transactions on Geoscience and Remote Sensing* 36
595 (6), 1945-1952.

596 Chanussot, J., Bas, P., Bombrun, L., 2005. Airborne Remote Sensing of Vineyards for the
597 Detection of Dead Vine Trees. In: *Proceedings IEEE International Geoscience & Remote*
598 *Sensing Symposium, Seoul, Korea*, pp.3090- 3093.

599 Chica-Olmo, M., Abarca-Hernández, F., 2000. Computing geostatistical image texture for
600 remotely sensed data classification. *Computers & Geosciences* 26, 373-383.

601 Congalton, R., 1991. A review of assessing the accuracy of classifications of remotely sensed
602 data. *Remote Sensing of Environment* 37 (1), 35-46.

603 Debeir, O., Van den Steen, I., Latinne, P., Wolff, E., Van Ham, Ph., 2002. Spectral, spatial and
604 contextual land cover classification using single and multiple classifiers. *Photogrammetric*
605 *Engineering & Remote Sensing* 68 (6), 597-605.

606 Durrieu, M., Ruiz, L.A., Balaguer, A., 2005. Analysis of geostatistical parameters for texture
607 classification of satellite images. In: *Proceedings EARSeL Symposium - Global Developments*
608 *in Environmental Earth Observation from Space, Porto, Portugal*, pp.11-18.

609 Fernández-Sarría, A., 2007. Estudio de técnicas basadas en la transformada wavelet y
610 optimización de sus parámetros para la clasificación por texturas de imágenes digitales. PhD
611 Dissertation, Universidad Politécnica de Valencia, Spain, 247 pp.

612 Ferro, C.J., Warner, T.A., 2002. Scale and texture in digital image classification.
613 *Photogrammetric Engineering & Remote Sensing* 68 (1), 51-63.

614 Gée, Ch., Bossu, J., Jones, G., Truchetet, F., 2008. Crop/weed discrimination in perspective
615 agronomic images. *Computers and Electronics in Agriculture* 60 (1), 49–59.

616 Gougeon, F., 1999. Automatic individual tree crown delineation using a valley-following
617 algorithm and a rule-based system. In: *Proceedings International Forum of Automated*
618 *Interpretation of High Spatial Resolution Digital Imagery for Forestry, Victoria, BC*, pp. 11–23.

619 Haralick, R.M., Shanmugam, K., Dinstein, I., 1973. Texture features for image classification.
620 *IEEE Transactions on Systems, Man and Cybernetics* 3 (6), 610-622.

621 Hay, G.J., Castilla, G., 2006. Object-based image analysis: strengths, weakness, opportunities
622 and threats (SWOT). *International Archives of the Photogrammetry, Remote Sensing and*
623 *Spatial Information Sciences XXXVI - 4/C42 on CD*.

624 Helmholtz, P., Gerke, M., Heipke, C., 2007. Automatic discrimination of farmland types using
625 Ikonos imagery. In: *Proceedings Photogrammetric Image Analysis 07, Munich, Germany*, pp.
626 81-86.

627 Hermosilla, T., Díaz-Manso, J.M., Ruiz, L.A., Recio, J.A., Fernández-Sarría, A., Ferradáns-
628 Nogueira, P., 2010. Parcel-based image classification as a decision-making supporting tool for
629 the Land Bank of Galicia (Spain). *International Archives of the Photogrammetry, Remote*
630 *Sensing and Spatial Information Sciences XXXVIII-4-8-2-W9*, 40-45.

631 Hoffer, R.M., 1975. Natural resource mapping in mountainous terrain by computer analysis of
632 ERTS-1 Satellite Data. LARS Information Note 061575, Purdue University, Indiana, 124 pp.

633 Hough, P.V.C., 1962. Methods and means for recognizing complex patterns, U.S. Patent No.
634 3069654.

635 Huang, X., Jensen, J.R., 1997. A machine-learning approach to automated knowledge-base
636 building for remote sensing image analysis with GIS data. *Photogrammetric Engineering &*
637 *Remote Sensing* 63 (10), 1185-1194.

638 Hutchinson, C.F., 1982. Techniques for combining Landsat and ancillary data for digital
639 classification improvement. *Photogrammetric Engineering & Remote Sensing* 48 (1), 123-130.

640 Jakomulska, A., Clarke, K.C., 2000. Variogram-derived measures of textural image
641 classification. Application to large scale vegetation mapping. In: *Proceedings Third European*
642 *Conference on Geostatistics for Environmental Applications geoENV2000*, Avignon, France,
643 pp. 181-202.

644 Janssen, L.L.F., Molenaar, M., 1995. Terrain objects, their dynamics and their monitoring by
645 the integration of GIS and remote sensing. *IEEE Transactions on Geoscience and Remote*
646 *Sensing* 33 (3), 749-758.

647 Krummel, J. R., Gardner, R. H., Sugihara, G., O'Neill, V., Coleman, P. R., 1987. Landscape
648 patterns in a disturbed environment. *OIKOS* 48 (3), 321-324.

649 Leemans, V., Destain, M.-F., 2006. Application of the Hough transform for seed row
650 localisation using machine vision. *Biosystems Engineering* 94 (3), 325–336.

651 Maillard, P., 2003. Comparing texture analysis methods through classification.
652 Photogrammetric Engineering & Remote Sensing 69 (4), 357-367.

653 Mallat, S.G., 1989. A theory of multiresolution signal decomposition: The wavelet
654 representation. IEEE transactions on pattern analysis and machine intelligence 11 (7), 674-693.

655 Mas, J.F., 2003. An artificial neural networks approach to map land use/cover using Landsat
656 imagery and ancillary data. In: Proceedings IEEE International Geosciences & Remote Sensing
657 Symposium, Toulouse, France, pp. 3498-3500.

658 McGarigal, K., Marks, B. J., 1995. FRAGSTATS: spatial pattern analysis program for
659 quantifying landscape structure. General Technical Report PNW-GTR-351. Portland, OR: U.S.
660 Department of Agriculture, Forest Service, Pacific Northwest Research Station. 122 pp.

661 Meinel, G., Neubert, M., 2004. A comparison of segmentation programs for high resolution
662 remote sensing data. International Archives of the Photogrammetry, Remote Sensing and
663 Spatial Information Sciences XXXV-B4, 1097-1102.

664 Neubert, M., Herold, H., 2008. Assessment of remote sensing image segmentation quality.
665 International Archives of the Photogrammetry, Remote Sensing and Spatial Information
666 Sciences XXXVIII-4/C1 on CD.

667 Pedley, M.I., Curran, P.J., 1991. Per-field classification: an example using SPOT-HRV imagery.
668 International Journal of Remote Sensing 12 (11), 2181-2192.

669 Pyrcz, M. J., Deutsch, C. V., 2003. The whole story on the hole effect. In: Searston, S. (Eds.)
670 Geostatistical Association of Australasia Newsletter 18.

671 Randen, T., Husoy, J.H., 1999. Filtering for texture classification: A comparative study. IEEE
672 Transactions on Pattern Analysis and Machine Intelligence 21 (4), 291-310.

673 Recio, J., 2009. Técnicas de extracción de características y clasificación de imágenes orientada
674 a objetos aplicadas a la actualización de bases de datos de ocupación del suelo. PhD
675 Dissertation. Universidad Politécnica de Valencia, Spain, 289 pp.

676 Recio, J.A., Hermosilla, T., Ruiz, L.A., Fernández-Sarría, A., 2009. Analysis of the addition of
677 qualitative ancillary data on parcel-based image classification. International Archives of the
678 Photogrammetry, Remote Sensing and Spatial Information Sciences XXXVIII-1-4-7/W5 on
679 CD.

680 Recio, J.A., Ruiz, L.A., Fernández-Sarría, A., Hermosilla, T., 2006. Integration of multiple
681 feature extraction and object oriented classification of aerial images for map updating. In:
682 Proceedings Second International Symposium on Recent Advances in Quantitative Remote
683 Sensing, Torrent, Spain, pp. 391-396.

684 Recio, J.A., Hermosilla, T., Ruiz, L.A., Fernández-Sarría, A., 2010. Addition of geographic
685 ancillary data for updating geo-spatial databases. International Archives of the Photogrammetry,
686 Remote Sensing and Spatial Information Sciences XXXVIII-4-8-2-W9, 46-51.

687 Reid, J.F., Searcy, S.W., 1986. Detecting crop rows using the Hough transform. ASAE Paper
688 No. 86-3042, St. Joseph, MI, USA.

689 Rogan, J., Miller, J., Stow, D., Frankling, J., Levien, L., Fischer, C., 2003. Land cover change
690 mapping in California using classification trees with multitemporal Landsat TM and ancillary
691 data. Photogrammetric Engineering & Remote Sensing 69 (7), 793-804.

692 Ruiz, L.A., Fernández-Sarría, A., Recio, J., 2002. Evaluation of texture analysis techniques to
693 characterize vegetation. In: Proceedings International Symposium on Recent Advances in
694 Quantitative Remote Sensing, Torrent, Spain, pp. 514-521.

695 Ruiz, L.A., Fernández-Sarría, A., Recio, J.A., 2004. Texture feature extraction for classification
696 of remote sensing data using wavelet decomposition: A comparative study. International

697 Archives of the Photogrammetry, Remote Sensing and Spatial Information Sciences, XXXV-
698 B4, 1109-1114.

699 Ruiz, L.A., Recio, J.A., Hermosilla, T., 2007. Methods for automatic extraction of regularity
700 patterns and its application to object-oriented image classification. International Archives of the
701 Photogrammetry, Remote Sensing and Spatial Information Sciences XXXVI-3/W49A, 117-121.

702 Ruiz, L.A., Recio, J.A, Hermosilla, T., Fernández-Sarría, A., 2009. Identification of agricultural
703 and land cover database changes using object-oriented classification techniques. In: Proceedings
704 33rd International Symposium on Remote Sensing of Environment, Stresa, Italy, on CD.

705 Shapiro, L.G., Stockman, G.C., 2001. Computer Vision, Prentice-Hall, New Jersey, 580 pp.

706 Simard, M., DeGrandi, G., Thomson, K.P., 1999. Adaptation of the wavelet transform for the
707 construction of multiscale texture maps of SAR images. Canadian Journal of Remote Sensing
708 24 (3), 264-285.

709 Smith, G., Morton, D., 2008. Segmentation: The Achilles heel of object-based image analysis?.
710 International Archives of the Photogrammetry, Remote Sensing and Spatial Information
711 Sciences, XXXVIII-4/C1 on CD.

712 Sutton, R.N., Hall, E.L., 1972. Texture measures for automatic classification of pulmonary
713 disease. IEEE Transactions on Computers 21 (7), 667-676.

714 Trías-Sanz, R., 2006. Texture orientation and period estimation for discriminating between
715 forests, orchards, vineyards, and tilled fields. IEEE Transactions on Geoscience and Remote
716 Sensing 44 (10), 2755-2760.

717 Van Coillie F.M.B., Pires, P.L.V.M., Van Camp, N.A.F, Gautama, S., 2008. Quantitative
718 segmentation evaluation for large scale mapping purposes. International Archives of the
719 Photogrammetry, Remote Sensing and Spatial Information Sciences, XXXVIII-4/C1 on CD.

720 Van de Wouwer, G., Scheunders, P., Van Dyck, D., 1999. Statistical texture characterization
721 from discrete wavelet representations. *IEEE Transactions on Image Processing* 8 (4), 592-598.

722 Volante, J. N., Campos, C. J., Noé, Y. E., Elena, H. J., 2007. Método de clasificación "por
723 parcela" para la detección de cultivos: Aplicación al área agrícola de Las Lajitas (Salta,
724 Argentina), (Per-field classification method to detect crops: Application in agricultural area of
725 Las Lajitas (Salta, Argentina)). In: *Proceedings XII Congress Remote Sensing Spanish*
726 *Association, Mar del Plata, Argentina*, pp. 79-86.

727 Walker, J.S., 1999. *A Primer on Wavelets and their Scientific Applications*, 1st edn., Chapman
728 & Hall/CRC, Boca Raton, FL, 155 pp.

729 Walter, V., 2004. Object-based classification of remote sensing data for change detection.
730 *ISPRS Journal of Photogrammetry and Remote Sensing* 58 (3-4), 225-238.

731 Woodcock, C.E., Strahler, A.H., Jupp, D.L.B., 1988a. The use of variograms in remote sensing
732 I: Scene models and simulated images. *Remote Sensing of Environment* 25 (3), 323-348.

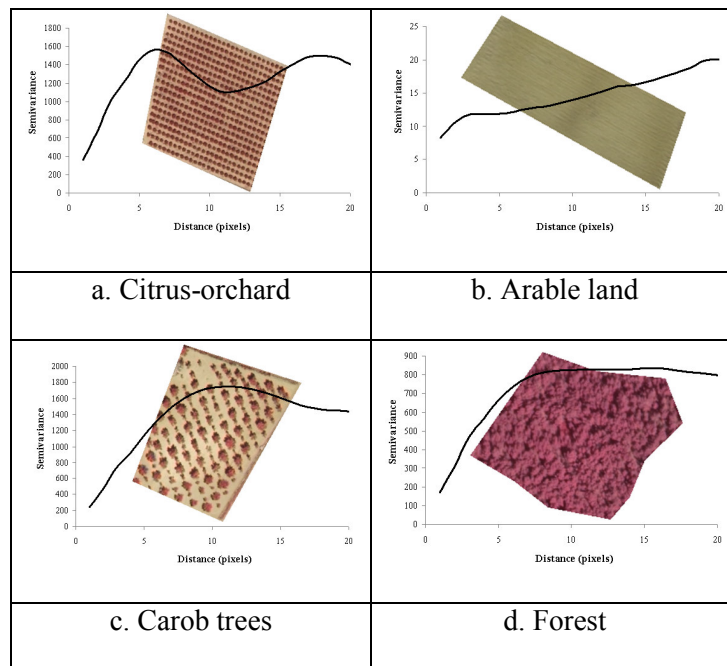
733 Woodcock, C.E., Strahler, A.H., Jupp, D.L.B., 1988b. The use of variograms in remote sensing
734 II: real digital images. *Remote Sensing of Environment* 25 (3), 349-379.

735 Wulder, M., Niemann, K.O., Goodenough, G.D., 2000. Local maximum filtering for the
736 extraction of tree locations and basal area from high spatial resolution imagery. *Remote Sensing*
737 *of Environment* 73 (1), 103-114.

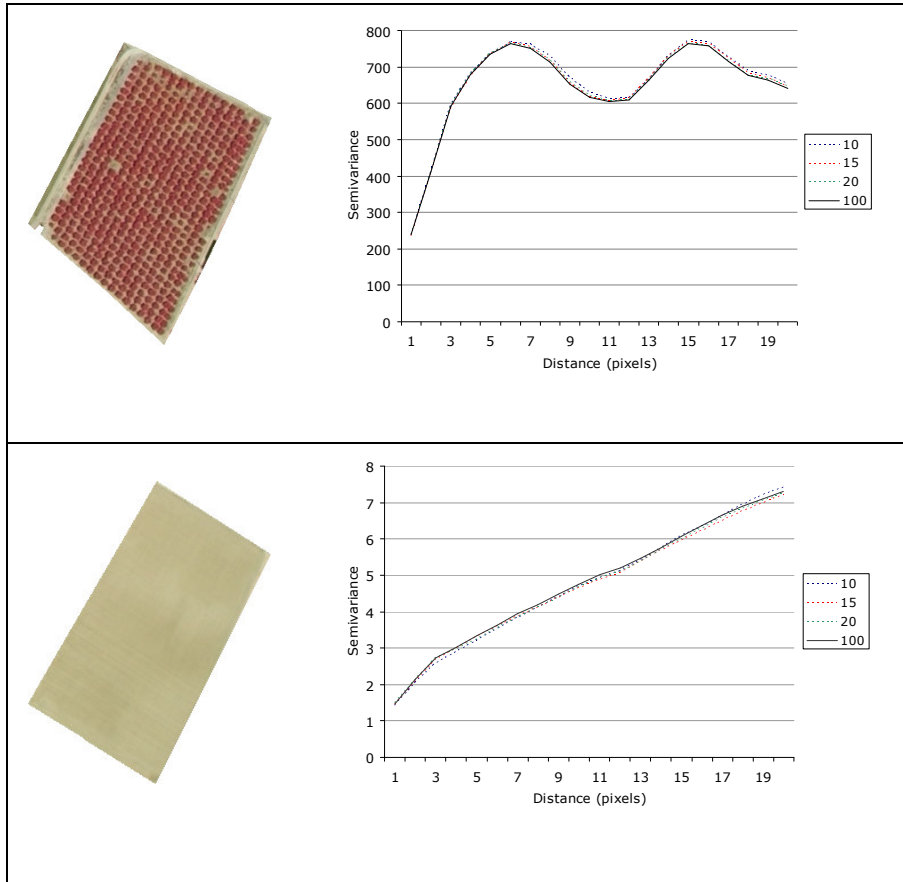
738 Zhang, H., Fritts, J.E., Goldman, S.A., 2008. Image segmentation evaluation: A survey of
739 unsupervised methods. *Computer Vision and Image Understanding* 2 (110), 260–280.

740 **Annexe: Description and codification of the features extracted by FETEX 2.0**

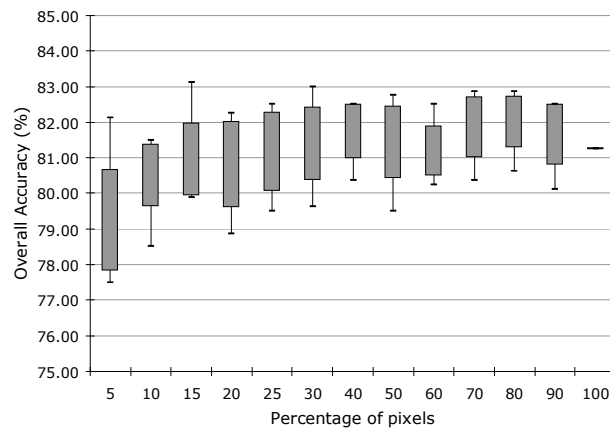
Spectral Features (number indicates the band)		Hough transform features	
MEAN1	Mean value of band 1	ANG_DIF	Angular difference between the two principal directions
STDEVI	Standard deviation value of band 1	ANG1PERC	Proportion of straight lines in the principal direction
MIN1	Minimum value of band 1	ANG2PERC	Proportion of straight lines in the secondary direction
MAX1	Maximum value of band 1	RHO1MEAN	Mean of the distances between straight lines in the principal direction
RANGE1	Range of values of band 1	RHO1 STDEV	Standard deviation of the distances between straight lines in the principal direction.
SUM1	Summatory of values of band 1	PT1PERC	Proportion of points included in the principal direction
MAJORITY1	Mode of values of band 1	PT1NORM	Proportion of points included in the principal direction normalized by area
MEANNDVI	Mean value of NDVI	RHO1MEDIAN	Median of the distances between straight lines in the principal direction
STDEVNDVI	Standard deviation value of NDVI	RHO2MEAN	Mean of the distances between straight lines in the secondary direction
MINNDVI	Minimum value of NDVI	RHO2 STDEV	Standard deviation of the distances between straight lines in the secondary direction.
MAXNDVI	Maximum value of NDVI	PT2PERC	Proportion of points included in the secondary direction
RANGENDVI	Range of values of NDVI	PT2NORM	Proportion of points included in the secondary direction normalized by area
SUMNDVI	Summatory of values of NDVI	RHO2MEDIAN	Median of the distances between straight lines in the secondary direction
Texture Features		Semivariogram based features	
MEAN_EDG	Mean value of edgeness factor	RVF	Ratio between the values of the total variance and the semivariance at first lag
STDEV_EDG	Standard deviation of edgeness factor	RSF	Ratio between semivariance values at second and first lag
UNIFOR	GLCM Uniformity	FDO	First derivative near the origin
ENTROP	GLCM Entropy	FML	First maximum lag value
CONTRAS	GLCM Contrast	MFM	Mean of the semivariogram values up to the first maximum
IDM	GLCM Inverse Difference Moment	VFM	Variance of the semivariogram values up to the first maximum
COVAR	GLCM Covariance	RMM	Ratio between the semivariance at first local maximum and the mean semivariogram values up to this maximum
VARIAN	GLCM Variance	DMM	Distance between the first maximum and the first minimum
CORRELAT	GLCM Correlation	Shape features	
SKEWNESS	Skewness value of the histogram	COMPACT	Compactness
KURTOSIS	Kurtosis value of the histogram	SH_INDEX	Shape Index
Wavelet based features		FRACTAL	Fractal dimension
MEAN_W1	GLCM Mean of the details image	AREA	Area
UNIFOR_W1	GLCM Uniformity of the details image	PERIMETER	Perimeter
ENTROP_W1	GLCM Entropy of the details image	Ancillary data features	
CONTRAS_W1	GLCM Contrast of the details image	ANCILLARY	Ancillary data from database
IDM_W1	GLCM Inverse Difference Moment of the details image	Processing information	
COVAR_W1	GLCM Covariance of the details image	PROCESSED	Processing information
VARIAN_W1	GLCM Variance of the details image	Training sample identification	
CORRELAT_W1	GLCM Correlation of the details image	SAMPLE	Training sample class
MEAN_EDG_W1	Mean value of edgeness factor of the details image		
STDEV_EDG_W1	Standard deviation of edgeness factor of the details image		



743 Figure 1. Parcels with different land use and their respective experimental semivariogram
 744 superimposed. Distance in pixels is in abscissas, and semivariance values are represented in
 745 ordinates.

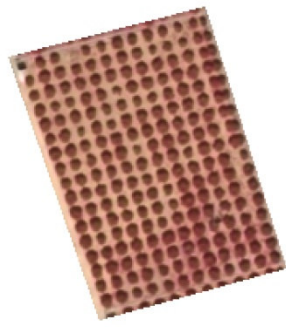


747 Figure 2. Semivariograms computed using different pixel percentages (10, 15 and 20) compared
 748 to semivariograms computed using all pixels in object.

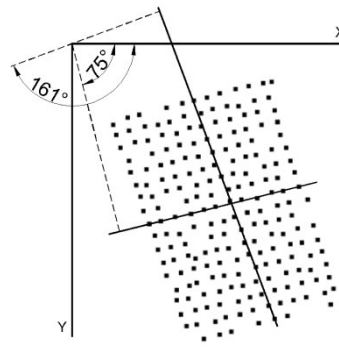


750

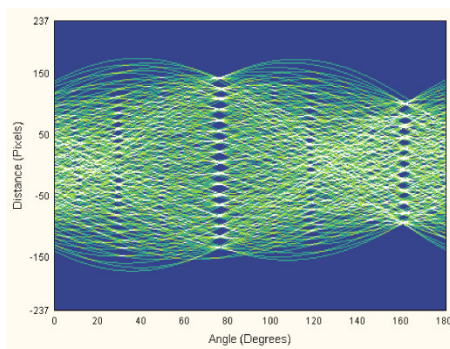
751 Figure 3. Box and whiskers graph representing overall accuracies of a series of 10
 752 classifications for each pixel percentage used to compute semivariogram. Whiskers represent
 753 maximum and minimum values; boxes represent one standard deviation apart from mean
 754 values.



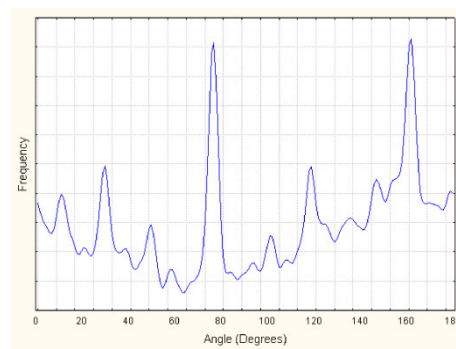
a.



b.



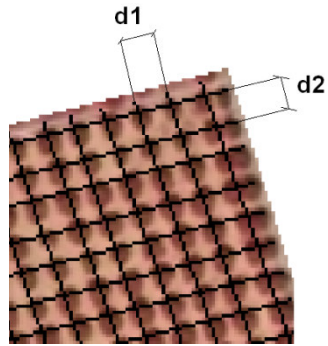
c.



d.

756 Figure 4. Example of application of the Hough transform method: (a) object in image space; (b)
 757 local maxima detection; (c) Hough transform space; (d) histogram of coincidences in different
 758 directions. Main directions are extracted at 75° and 161° .

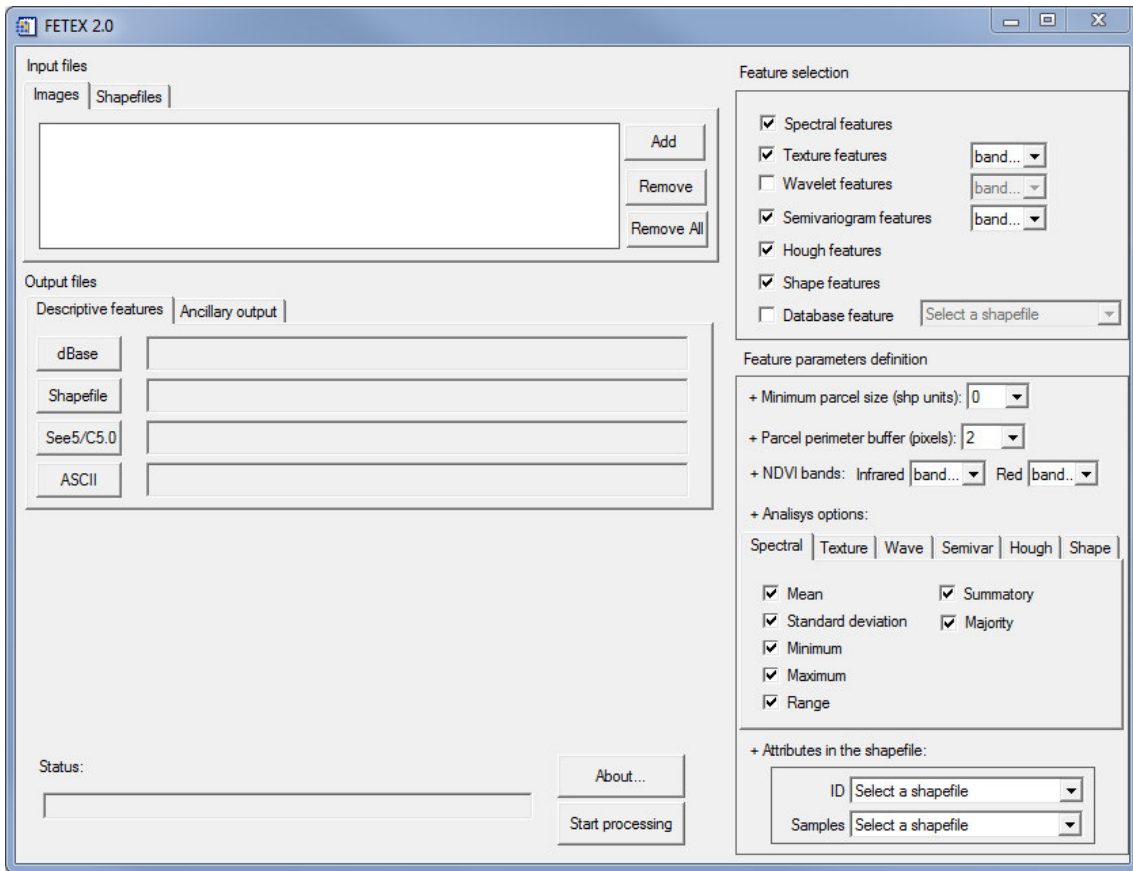
759



760

Figure 5. Extraction of planting pattern distances.

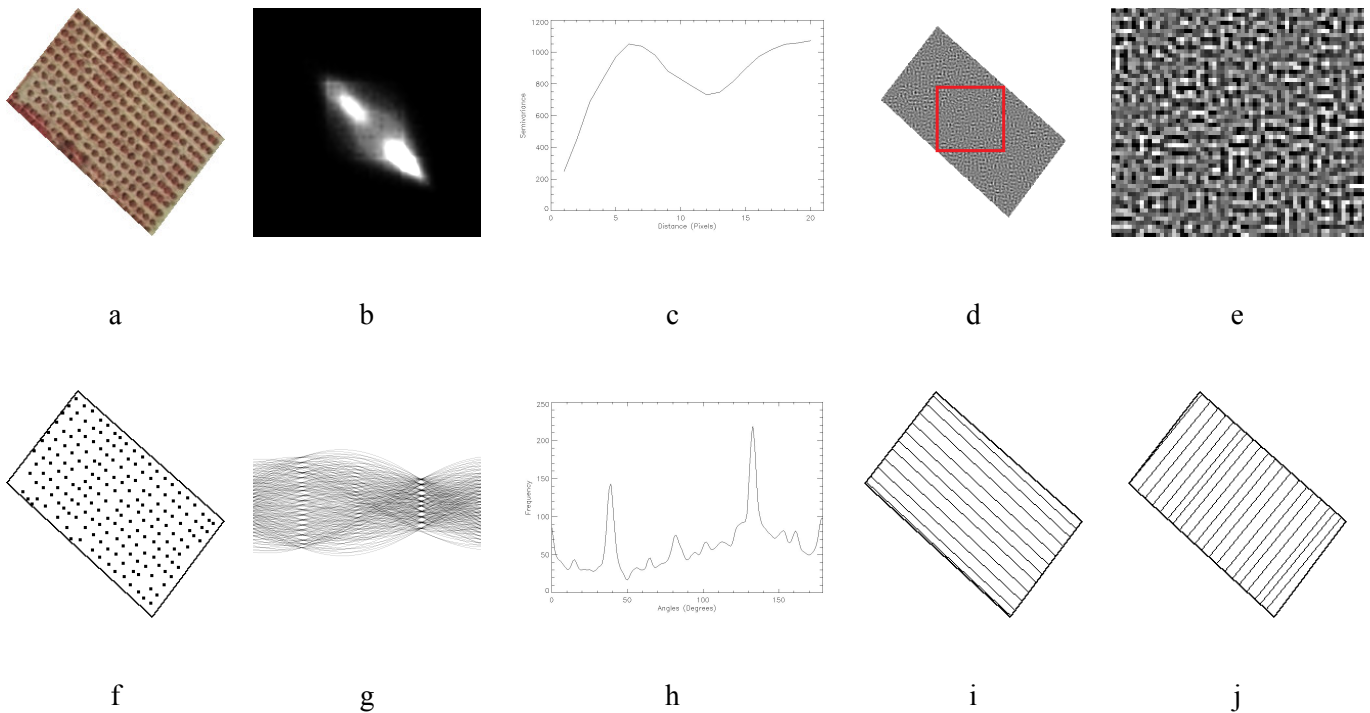
761



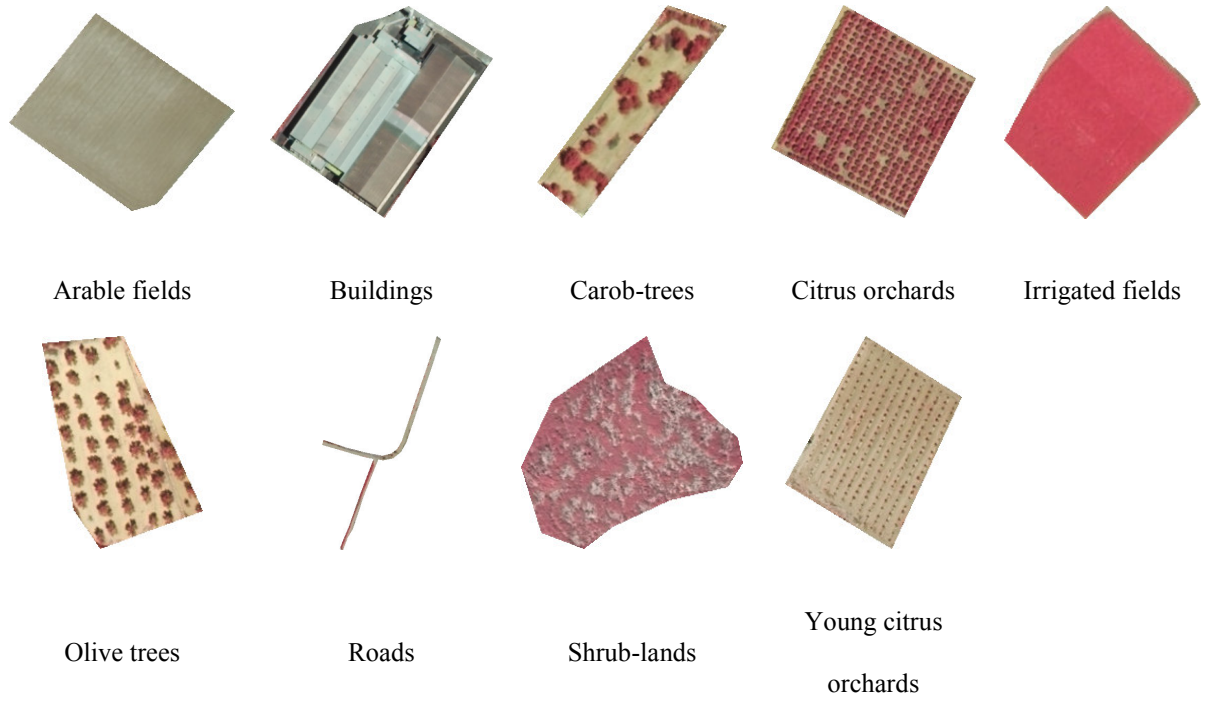
762

763

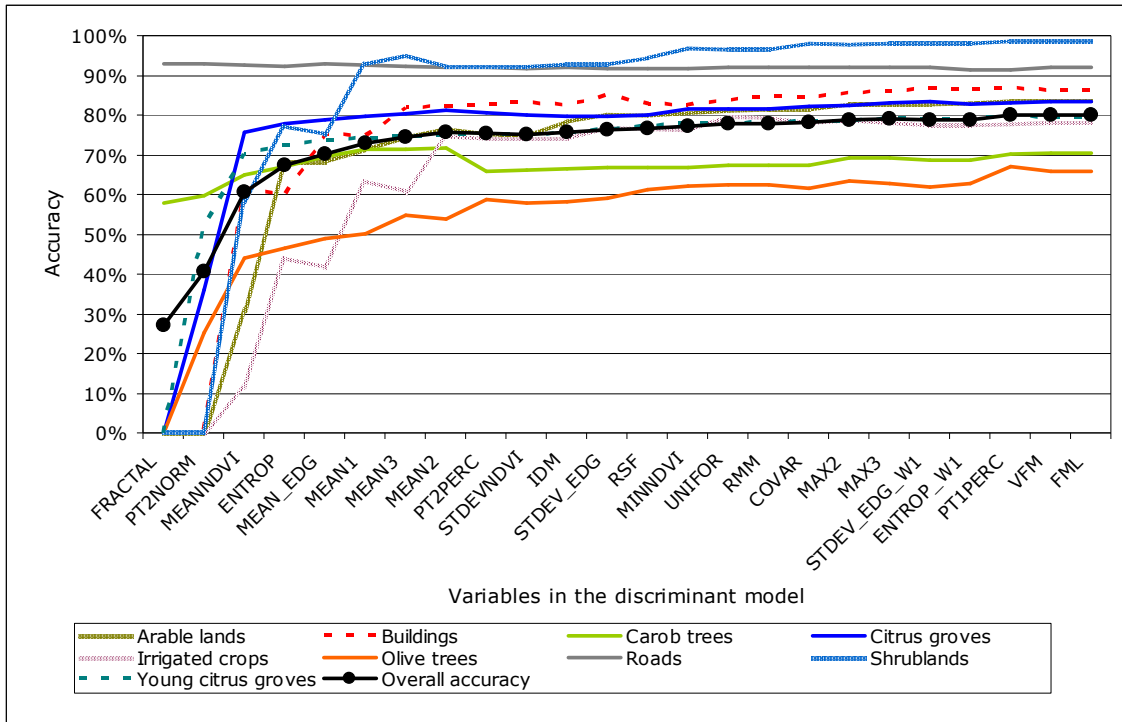
Figure 6. Graphic user interface of FETEX 2.0.



765 Figure 7. Examples of screenshots generated by FETEX 2.0 in a citrus crop parcel: (a) Color
 766 infrared image of object; (b) grey level image representation of the GLCM; (c) semivariogram
 767 graph (with *hole-effect* presence); (d) sum of details of wavelet decomposition (Coiflet, size 24
 768 pixels); (e) detail of (d); (f) local maxima detected representing trees; (g) Hough space
 769 representation of local maxima; (h) Hough transform directions histogram; (i) alignments in
 770 main direction; (j) alignments in second direction.



772 Figure 8.- Image-object examples, in color infrared composition, of classes considered for
773 classification.

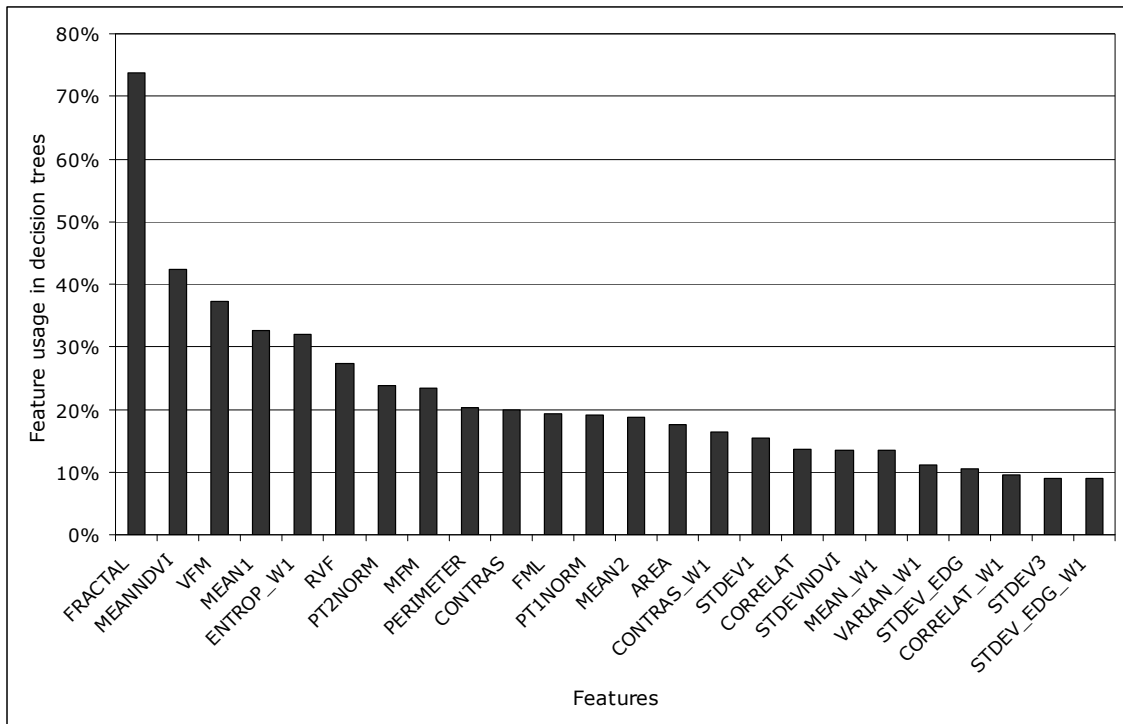


774

775 Figure 9.- Overall classification accuracy and *per-class* accuracies when new variables are

776

progressively included into the discriminant model.



777

778

Figure 10.- Feature percentage of use in decision tree construction.

Table 1.-Shape parameters computed in FETEX 2.0.

$$C = \frac{4 \cdot \pi \cdot Area}{Perimeter^2}$$

$$SI = \frac{Perimeter}{4 \cdot \sqrt{Area}}$$

$$FD = 2 \cdot \frac{\log\left(\frac{Perimeter}{4}\right)}{\log(Area)}$$

a. Compactness

b. Shape index

c. Fractal dimension

780 Table 2. Overall classification accuracies using different groups and combinations of
 781 descriptive features

Descriptive feature groups	Classification method	
	Linear discriminant analysis	Decision trees (C5.0)
Spectral features	65.5%	60.0%
Texture features	65.4%	66.7%
Structural features	57.8%	62.1%
Shape features	32.2%	35.4%
All features	81.7%	80.6%

782